'All in one' photo-reactor pod containing TiO2 coated glass beads and LEDs for continuous photocatalytic destruction of cyanotoxins in water.

GUNARATNE, H.Q.N., PESTANA, C.J., SKILLEN, N., HUI, J., SARAVANAN, S., EDWARDS, C., IRVINE, J.T.S., ROBERTSON, P.K.J. and LAWTON, L.A.

2020

Paper

'All in one' photo-reactor pod containing TiO₂ coated glass beads and LEDs for continuous photocatalytic destruction of cyanotoxins in water

H. Q. Nimal Gunaratne,[c] Carlos J. Pestana,[a] Nathan Skillen,[c] Jianing Hui,[b] S. Saravanan,[b] Christine Edwards,[a] John. T. S. Irvine,*[b] Peter. K. J. Robertson,*[c] and Linda A. Lawton,*[a]

Blooms of blue-green algae (cyanobacteria) in water reservoirs frequently produce highly toxic secondary metabolites including microcystins which have resulted in both human and animal fatalities. To tackle this global problem, we present here a viable solution: utilising the photo-catalytic power of TiO₂ immobilised on glass beads that are encased in 'photo-reactor pods', equipped with UV LEDs, for the photocatalytic destruction of cyanotoxins. These reactor pods are designed in such a way that they can be used continuously with the aid of a power supply to facilitate the photocatalytic process. This process could be used to address one of the Global Challenges: providing safe drinking water around the globe.

Much of the accessible freshwater has suffered from the effects of industrialisation and population over the last century. Polluting chemicals have degraded the quality of water as industrial discharge and wastewater have allowed chemicals to accumulate. Eutrophication, the enrichment of waterbodies with the nutrients (chiefly nitrate and phosphate), has been observed in many parts of the world because of agricultural run-off, industrial processes and domestic wastewater. Eutrophication is now regarded as one of the significant problems affecting freshwater bodies.[1] A direct correlation has been observed between rising nutrient levels and the occurrence of algal blooms which is responsible for lowering the water quality.[2] Algal blooms cause a number of problems including oxygen depletion, elevated organic carbon load, decrease in biodiversity and limited water transparency.[3] Blooms of blue-green algae (cyanobacteria) also very frequently produce highly toxic secondary metabolites including microcystins, saxitoxins, anatoxins and cylindrospermopsins which have resulted in both human and animal health issues.[4] Blue-green algal blooms and their toxins are of increasing global concern as they can dominate the

microflora of freshwater supplies and it is becoming apparent that climate change is exacerbating the situation.[5] Although these toxins have been detected in drinking water reservoirs in some parts of the world most conventional water treatment systems fail to remove them in the dissolved state and even advanced systems are known to experience breakthrough during times of high dissolved toxin influx.[6] We have extensively explored the application of the photocatalyst TiO₂ for the removal of a range of blue-green algal (cyanobacterial) toxins.[7] This advanced oxidation method has been found to very rapidly remove these compounds (c. 10 min) with no toxic by-products.[4-8] The toxins are destroyed by high energy OH· radicals produced when TiO₂ is excited by UV-light (see Figure 1A).
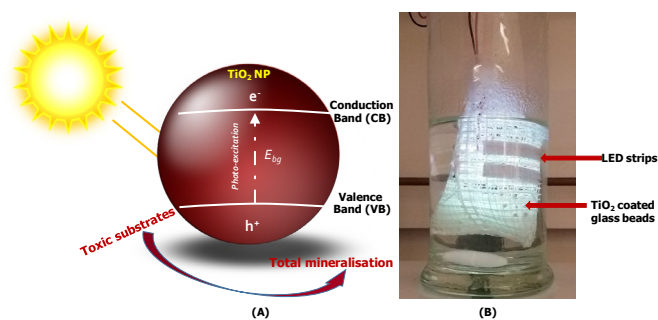

Figure 1: (A); Illustration of the 'hole forming' photochemical process of TiO₂ that is responsible for photo-catalytic destruction of toxic substrates such as microcystins; **(B)** our design of a pod with a LED attachment containing glass beads coated with TiO₂-NPs

This effective method of oxidising water contaminants allows the catalyst to be repeatedly activated with OH· radicals being continually generated without the addition of any further chemicals. In this communication, we present the design of a photochemical reactor pod with wired LED strips that houses TiO₂ coated glass beads for photo-catalytic destruction of undesirable compounds such as microcystins. The pod can be immersed in toxin containing water and operate continuously, removing these compounds very effectively from water.

a. School of pharmaceutical and life sciences, Robert Gordon University, Aberdeen, Scotland.
b. Department of Chemistry, St. Andrews University, Scotland
c. School of chemistry and chemical engineering, Queen's University Belfast, UK
† Footnotes relating to the title and/or authors should appear here.
Electronic Supplementary Information (ESI) available: Some UV-Visible spectra and additional reaction kinetic profiles are given in ESI. See DOI: 10.1039/x0xx00000x

We present here a model study on different pod designs where their performances were first assessed with organic dyes or sorbic acid as model substrates. Subsequently, microcystin-LR was used as a representative example of toxins that belongs to the class of microcystins having over 240 analogoues. The general structure of one such microcystin (LR) is shown in figure 2A. They are cyclic peptides with seven amino acids including the unique and conserved amino acid, Adda (2S,3S,8S,9S,)-3-amino-9-methoxy-2,6,8-trimethyl-10-phenyldeca-4,6-dienoic acid which contains an unconjugated diene. Microcystin-LR contains two carboxylic acid functionalities with one fully deprotonated due to the presence of guanidine unit. Carboxylic acids are known to have high affinity to TiO_2 surface *via* hydrogen bonding facilitating the more effective attack by the generated $HO^.$ radicals (see figure 2B).
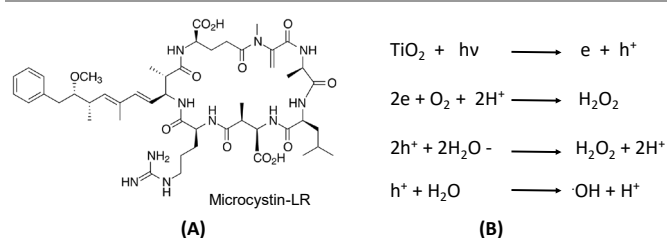

Figure 2: (**A**), Cyclic heptapeptide structure of microcystin-LR with a pendant diene, guanidine side chain and two carboxylic acid groups which have high affinity towards TiO_2; (**B**), established mechanism for photo-generated $OH^.$ radicals from TiO_2 with water and oxygen.

Several photoreactor pods, *viz* P1, P2, P3 and P4, iteratively designed for this work are shown in Figure 3. These reactor pods were wired with UV LED strips on the inner side and provide adequate space for accommodating any type of TiO_2 support materials. The supports that are used for depositing TiO_2-NPs are glass beads, glass wool and a glass fibre woven tape with some degree of porosity.
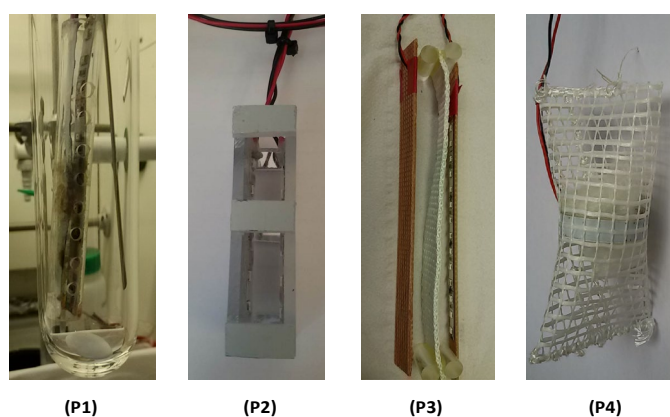

(P1)　　**(P2)**　　**(P3)**　　**(P4)**

Figure 3: P1 the inner perforated tube contains two LED strips with TiO_2 coated glass wool placed in between; **P2** rectangular shape pod, made of Perspex, with LED strips attached to inner walls where any TiO_2 supported materials can be housed; **P3** TiO_2 coated glass fibre tape placed between two UV LED strips; **P4** a pod made up of fibre glass mesh where wired UV LED strips are attached inside. TiO_2 coated glass beads or glass wool may be placed inside**.**

Initially, the photocatalytic performance of each pod was assessed by the degradation studies of organic dyes and other related substances (see Scheme 1). Moreover, different supports for TiO_2 were also assessed. It is common practice to use organic dyes for this evaluation process[9]. The degradation of dyes could easily and accurately be monitored by UV-Visible spectrometry due to their relatively high extinction coefficients. It is also established that toxicity of the microcystins is attributed to the outer tail motif bearing the conjugated diene. Therefore, apart from the standard dyes we also selected an organic compound with a diene motif and a carboxylic acid functionality, *viz*, sorbic acid.

Phenol red　　　**Methyl orange**　　　**Sorbic acid**
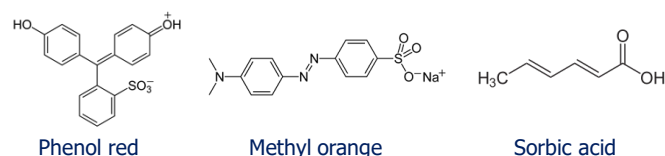
Scheme 1: Compounds used for the photocatalytic degradation study

In pod P1, the photocatalytic degradation of methyl orange was carried out utilising TiO_2 deposited on glass wool where the reaction was monitored by UV-Visible spectrometry. The reaction profile with time is depicted in Figure 4. The visible band centred at 465, characteristic of methyl orange, decline with time, when the illuminated pod P1 (with TiO_2 coated glass wool) was immersed in the aqueous dye solution.
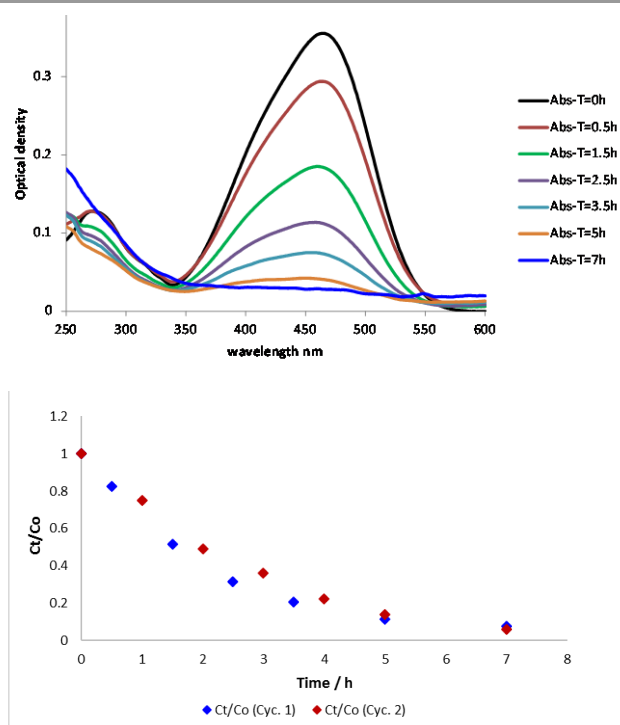

Figure 4: (A), Degradation of the methyl orange dye is seen, with time, by the demise of the absorption band centred at 465 nm; **(B),** red and blue curves show the kinetic profile for two repeated cycles using the TiO_2 supported glass wool. C_t and C_o refer to OD (465 nm) at time=t and time=0, respectively

The two repeated cycles with the same pod/coated material gave very similar results, as seen from figure 4B, indicating the recyclability of our system. This was further supported by the fact that same pod P1 system when used in another experiment where it was immersed in an aqueous dye solution of phenol red, the degradation occurred efficiently (see ESI-figure S1). Our notion of the ability to use these pods continuously, immersed in a water medium, remains justified. TiO_2 was coated on glass wool using a standard sol-gel solution of titania[10] and then heated to 550 °C to facilitate the activation. This TiO_2 coated glass wool was characterised by SEM and EDX spectroscopy (see Figure 5).
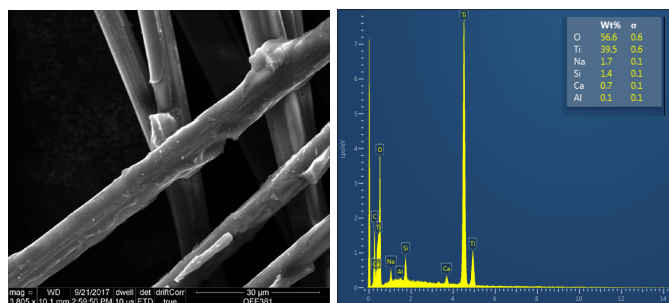

Figure 5: On the left: SEM image of TiO_2 coated glass wool; **on the right**: EDX analysis of the glass wool indicating high content of deposited photocatalyst.

Moreover, no shedding of the photocatalyst from glass wool surface was observed, even after several photocatalytic cycles indicating the robustness of the adhesion of TiO_2 on amorphous glass.[11] The pod P2 was assessed similarly using the same batch of TiO_2 coated glass wool. For all three model compounds given in scheme 1, very similar photocatalytic degradation results were obtained, as in the case of pod 1 (see ESI figures S2 and S3 for details). The 'open nature' of the design of pod 2 does not warrant the use of other supports like glass beads. Next, we examine the performance of pod 3 where the design and the support for TiO_2 was distinctly different in comparison to P1 and P2. Tightly woven fibre glass tape was utilised as the support for TiO_2. The deposition of TiO_2 on the glass tape was carried out utilising the same protocol as the one used for glass wool and the thermal activation procedure is also the same. The flexibility of the fibre glass tape remained unaffected after the deposition of TiO_2. The characterisation of the glass tape was carried by removing a few strands of fibres and subjecting it to SEM and EDX spectroscopy. The EDX analysis is given in figure 6 which indicates the presence of a reasonably high loading of titanium on the surface of the fibre glass tape.
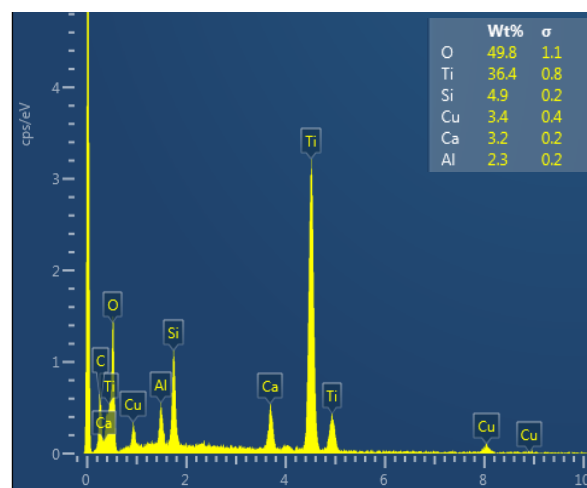

Figure 6: The EDX analysis of few fibre glass threads taken from the TiO_2 coated glass tape.

The photocatalytic activity of the tape assessed by the degradation efficiency of sorbic acid in an aqueous solution where the photo-destruction was monitored by UV spectrometry (see figure 7). The degradation kinetics were followed by monitoring the reduction of the UV-band at 255 nm.

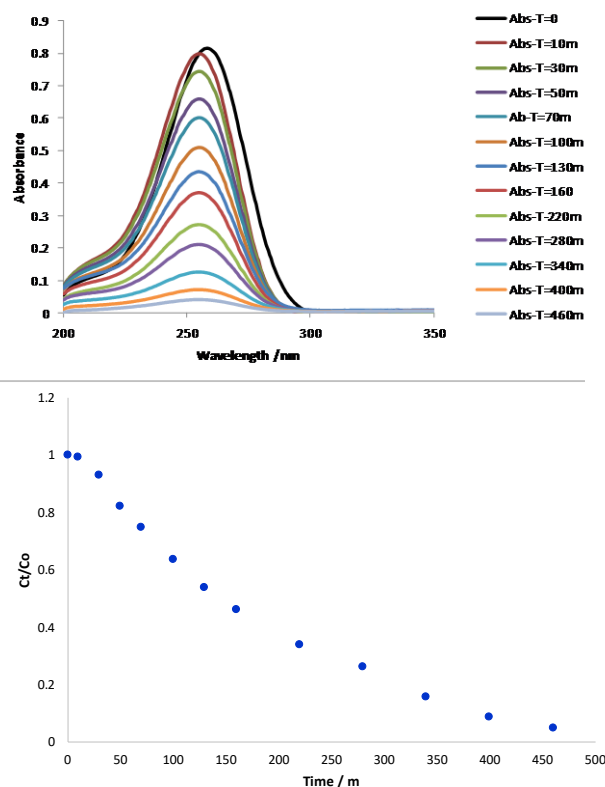**Figure 7: Top**: collection of UV spectra recorded at various times while irradiating an aqueous sorbic acid solution with the pod 3 carrying a TiO_2 coated glass tape immersed in it. Initial [Sorbic acid] = 3.478×10^{-5} M; **Bottom:** Degradation kinetic of sorbic acid as seen by the reduction of the UV band at 255 nm. Ct and Co refer to OD (256 nm) at time=t and time=0, respectively

It is noteworthy that the set of UV spectra obtained for the destruction of sorbic acid show no well-defined isosbestic points[12] suggesting the identifiable products formed in photodissociation process are further decomposed swiftly into unidentifiable products. Judging from the previous body of work on TiO_2 catalysed photo-dissociation of organic substances[13], it is plausible to assume the occurrence of full mineralisation of sorbic acid. Mechanistically, an initial attack of the photo-generated HO⋅ radical on the alkene function of sorbic acid can be envisaged. The resulting (multi-)hydroxyl functionalised compounds could be further attacked by the hydroxyl radicals leading to full mineralisation. Some evidence for the initial formation of hydroxylated compounds can be obtained by a ^1H NMR spectroscopic analysis of a D_2O solution of sorbic acid when subjected to TiO_2 (P25) catalysed photolysis. A ^1H NMR stack plot is shown in figure 8 where the photolysis was monitored by NMR at different time intervals. The NMR signals belonging to olefinic protons of sorbic acid disappears within 1 hour. The signal at δ 1.7 that belongs to the methyl group in sorbic acid is shifted upfield to δ 1.25 indicating the loss of double bonds. Moreover, the appearance of new peaks around δ 5.6 is also indicative of the presence of -CH-OH functionalities[14]. Continued irradiation of 4h resulted in almost complete disappearance of all peaks, indicating full mineralisation. Even though, sorbic acid has no direct similarity to the complex structures of microcystins, it carries a diene motif and a carboxylic acid functionality which are common to all microcyctins. This NMR study also shed some light into the photo-destruction reaction.
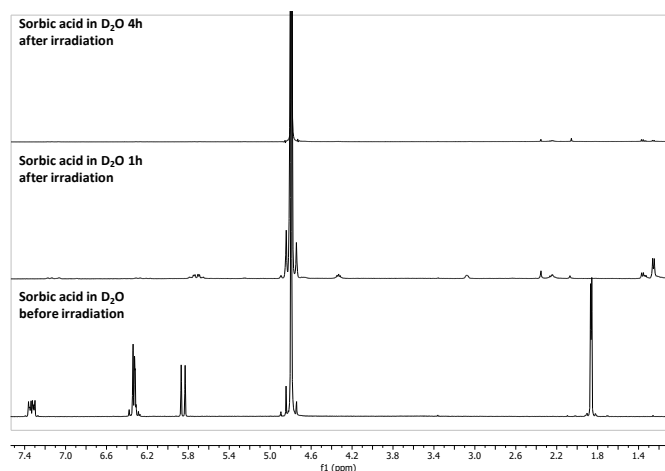

Figure 8: 400 MHz Partial ^1H NMR spectra of sorbic acid, in D_2O, before and after photolysis (1h and 4h; as shown in the figure) catalysed by TiO_2 (P25); [sorbic acid] = 12 mM, 6.1 mg of P25 used.

Unlike pods P1, P2 and P3, the pod P4 made from the fibre glass mesh was able to house the TiO_2 coated glass beads with some degree of buoyancy. A similar analysis that was carried out for other pods was performed on the Pod 4. Activity was measured using dyes and sorbic acid degradation. The coated glass beads were fully characterised by SEM and EDX spectroscopy (see figure 9).
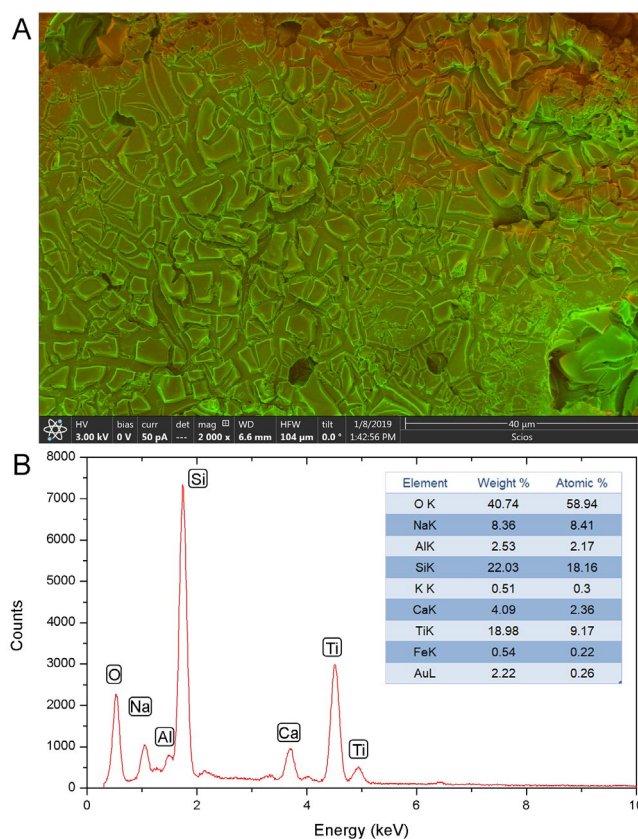

Figure 9: (A) SEM image coated beads show uniformly immobilized TiO_2 film; (B) EDX analysis of TiO_2 coated glass beads.

As shown in Figure 9A, a film of TiO_2 distributed on the glass beads' surface uniformly. The binding between TiO_2 coating and glass beads appears stable, although the film cracked during annealing. The fact, that no shedding of catalyst was observed in the catalytic test illustrates the robustness of the coating film. Ti peaks present in EDX spectrum in Figure 9B confirm the existence of TiO_2. The elemental quantity counting shows the weight percentage of TiO_2 is about 32% on the glass beads surface.

Even though photodegradation of dyes and sorbic acid occurred in all 4 pods, the designs of P1, P2 and P3 were not suitable to house TiO_2 coated glass beads. Moreover, as far as the supports for TiO_2 was concerned, the fragility of glass wool deemed unsuitable due to safety concerns. The glass beads employed for the purpose of support for TiO_2 were robust and relatively inexpensive. It was observed no cloudiness in the solution indicating a negligible amount of shedding of the catalyst from the coated glass beads. Having taken into account all these factors, we have selected to perform the key experiments with toxins in P4 with TiO_2 coated glass beads.

Finally, we carried out a performance study on the pod 4, containing aforementioned glass beads, by monitoring the photodegradation of the model compounds given in scheme 1. As expected, not only efficient degradation of sorbic acid and

others occurred on illumination by the 'in-house' LED strips but also robust reusability of the system was demonstrated. The results obtained on photocatalytic degradation of sorbic acid, including reuse/recycling of pod/beads, using pod 4 is summarised in figure 10 (see ESI for similar results on dye degradation with pod 4). Reuse/recycling experiments exemplify the longevity of our photocatalytic degradation system. With all these analyses, we have clearly demonstrated the versatility of the TiO_2 supported materials and the inbuilt LED system in comparison to experiments done with suspended TiO_2 powder in water with external illumination.[15]

much higher than the its levels expected to be present in general water bodies. The photocatalytic destruction of microcystin-LR was monitored by HPLC equipped with a photodiode array detector. The kinetic profile of the photo-decomposition is depicted in figure 11. Previously, microcystin-LR was photocatalytically destroyed by employing TiO_2 *nano*-powder (P25)[18] that was suspended in an aqueous solution where recycling of the photocatalyst became cumbersome.[7] The activity of the supported system compares well to the parent system with an added advantage of being able to reuse/recycle in a straightforward manner.

Figure 11: The kinetic profile of photocatalytic degradation microcystin-LR (1mg in 200 cm³ of artificial fresh water) performed with pod 4 containing TiO_2 coated glass beads. The loading of TiO_2 is 250 mg per 1g of coated glass beads. The LED array was operated at V_F = 12 dcV and I_F = 0.09 A (1.1 W). The delay time for dark absorption was 10 min.
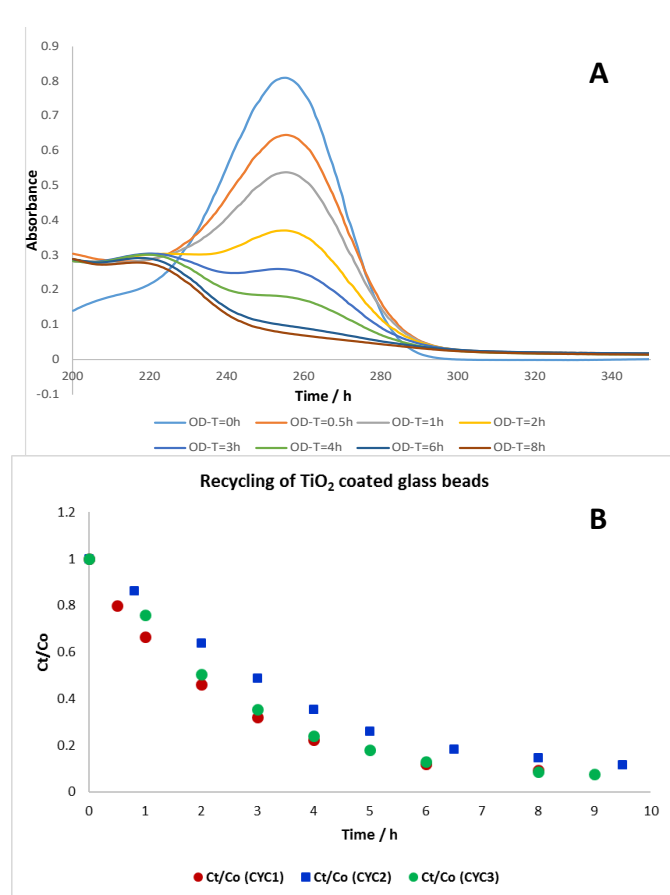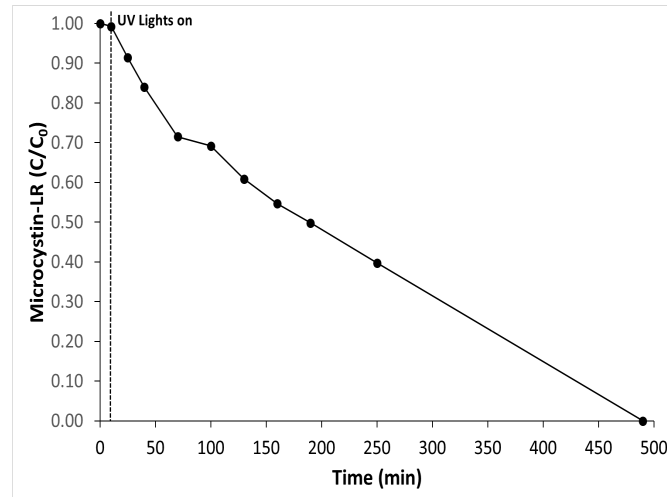

Figure 10: (A), a set of UV-spectra obtained for the 1st run of sorbic acid degradation utilising pod 6 with glass beads. Initial [Sorbic acid] = 3.488x10⁻⁵ M; **(B),** kinetic profiles of 3 photocatalytic degradation runs carried out with pod 4 with the same coated glass beads. Ct and Co refer to OD (256 nm) at time=t and time=0, respectively

Conclusions

In conclusion, we have developed an unprecedented photocatalytic reactor system which can be deployed in water reservoirs to be used continuously facilitating the removal of cyanobacteria and related toxins from drinking water. We envisage the power for the reactor system may be harnessed by attaching them to floating solar panels. It is envisaged that the mixing would be realised by the natural movement of water in reservoirs. This process would be ideal for global regions with long sunshine hours. It has been shown here the availability of several choices of diverse and viable supports for the photocatalyst TiO_2 for the construction of pod photoreactor devices. All the supports for TiO_2 demonstrated their robustness and longevity in relation to their realistic use in water bodies. Effectively, we have presented a model system based on green chemistry and chemical engineering principles to address one of the key Global Challenges, *i.e.* providing clean and safe water globally.

Having carried out an extensive study with model compounds, we performed an experiment with the environmentally relevant microcystin-LR with pod 4 consisting of the same glass beads that were used for model compounds. The World Health Organisation (WHO) maximum allowable level for total microcystins is 1 μg/L in drinking water and 20 μg/L in recreational waters.[16] A recent study in England reports microcystin ranges in lakes and reservoirs ranging from low ng/L to several mg/L. [17] It should be stressed here that the concentration of microcystin-LR used in this experiment§ was

Conflicts of interest

There are no conflicts to declare.

Acknowledgements

Notes and references

§ Microcystin-LR reference material used in our experiments was isolated from pure *Microcystis aeruginosa* cultures using preparative HPLC achieving > 98 % purity.
§§

1   H. W. Paerl and V. J. Paul, *Water Res.,* 2012, **46**, 1349-1363
2   H. W Paerl and T. G. Otten, *Microb. Ecol.*, 2013, **65**, 995-1010
3   H. W. Paerl and J. Huisman, Science, 2008, 320, 57-58; J. Huisman, H. C. P. Matthijs and P. M. Visser, *Harmful Cyanobacteria* (Springer, Dordrecht, Netherlands, 2005); H. W. Paerl and R. S. Fulton III, in *Ecology of Harmful Marine Algae*, E. Graneli, J. Turner, Eds. (Springer, Berlin, 2006), 95–107; I. Chorus, J. Bartram, *Toxic Cyanobacteria in Water* (Spon, London, 1999);
4   L. Bláha, P. Babica, and B. Maršálek, *Interdiscip Toxicol*., 2009, **2**, 36–41; G. Zanchett and E. C. Oliveira-Filho, *Toxins*, 2013, 5, 1896–1917; D. Drobac, N. Tokodi, J. Simeunovic, V. Baltic, D. Stanic, and Z. Svircev, Arch. Ind. Hygiene and Toxicology, 2013, **64**, 305-315.
5   W. W. Carmichael, *Human Ecol. Risk Assess,* 2001, **7**, 1393-1407; H. W. Paerl, R. S. Fulton, P. H. Moisander and J. Dyble, *The Scientific world*, 2001, **1**, 76-113.
6   H. Almuhtaram, Y. Cui, A. Zamyadi, and R. Hofmann, *Toxins*, 2018, **10**, 430-445; W. J. Cosgrove and D. P. Loucks, *Water Resour. Res.,* 2015, 51, 4823-4839.
7   C. J. Pestana, C. Edwards, P. K. J. Robertson, L. A. Lawton, *J. Haz. Mat.*, 2015, **300**, 347-353; C. J. Pestana, P. K. J. Robertson, C. Edwards, W. Wilhelm, C. McKenzie, L. A. Lawton, *Chem. Eng. J*, 2014, **235**, 293-298; P. K. J. Robertson, J. M. C Robertson and D. W. Bahnemann, *J. Haz. Mat*., 2012, **210-211**, 161-171.
8   I. Liu, L. A. Lawton, D. W. Bahnemann, L. Liu, B. Proft and P. K. J. Robertson, *Chemosphere*, 2009, **76**, 549-553.
9   B. A. van Driel, P. J. Kooyman, K. J. van den Berg, A. Schmidt-Ott and J. Dik, *Microchemical J.*, 2016, **126**, 162–171; C. L. Bianchi, E. Colombo, S. Gatto, M. Stucchi, G. Cerrato, S. Morandi and V. Capucci, *Photochem. Photobiol. A: Chemistry*, 2014, **280**, 27-31.
10 A. Mills, N. Elliott, G. Hill, D. Fallis, J. R. Durrant, and R. L. Willis, *Photochem. Photobiol. Sci.*, 2003, 2, 591–596; M. Adams, N. Skillen, C. McCullagh, P. K. J. Robertson, *Appl. Cat B: Environmental*, 2013, **130–131**, 99–105;
11 D. L. Cunha, A. Kuznetsov, C. A. Achete, A. E. da Hora Machado, and M. Marques, *PeerJ*, 2018, 6: e4464; D. S. Kim and S.-Y. Kwak, *Environ. Sci. Technol.*, 2009, **43**, 148–151
12 Heinz-Helmut Perkampus, *UV-VIS Spectroscopy and Its Applications*, Springer Lab Manuals, 1992; K. Ichimura, *Chem. Lett.*, 2018, **47**, 1247–1250.
13 W. Y. Teoh, F. Denny, R. Amal, D. Friedmann, L. Madler and S. E. Pratsinis, *Topics in Catalysis*, 2007, **44**, 489-497.
14 *Handbook of Proton-nmr Spectra and Data*, Ed. Asahi Research Center Co. Ltd., Tokyo, 1987 *Elsevier Inc*.
15 K. Nakata and A. Fujishima, *J. Photochem. and Photobiol. C: Photochem. Rev.,* 2012, **13**, 169–189.
16 Guidelines for Drinking-Water Quality: Fourth Edition Incorporating the first addendum. World Health Organisation (WHO): Geneva, Switzerland, 2017; N. Gray, Algae and algal toxins. In *Drinking Water Quality: Problems and Solutions*, 2008 (*pp*. 210-216). Cambridge: Cambridge University Press. doi:10.1017/CBO9780511805387.012;
17 A. D. Turner, M. Dhanji-Rapkova, A. O'Neill, L. Coates, A. Lewis, and K. Lewis, *Toxins*, 2018, **10**, 39-68.
18 J. Schneider, M. Matsuoka, M. Takeuchi, J. Zhang, Y. Horiuchi, M. Anpo and D. W. Bahnemann, *Chem. Rev.,* 2014, **114**, 9919–9986; D. Graham, H. Kirsch, L. A. Lawton and P. K. J. Robertson, *Chemosphere*, 2010, 78, 1182-1185; P. K. J. Robertson, L. A. Lawton, B. Muench and J. Rouzade, *Chem. Commun.,* 1997, 393-394; Note: TiO_2 (P25) used in this work was supplied by *Evonic*.

1   **Electronic Supplementary Information**

2

3   **'All in one' photo-reactor pod containing TiO$_2$ coated glass beads and**

4   **LEDs for continuous photocatalytic destruction of cyanotoxins in water**

5   H. Q. Nimal Gunaratne, Carlos J. Pestana, Nathan Skillen, Jianing Hui, S. Saravanan, Christine

6   Edwards, John. T. S. Irvine,* Peter. K. J. Robertson,* and Linda A. Lawton,*

7   **Materials:**

8   Porous glass beads in diameter of 2~4 mm (Poraver, Germany) were employed as

9   substrate in this work. The average density of the glass beads is around 0.6 g cm^{-3}.

10   Titanium (IV) isopropoxide (Sigma-Aldrich, 97%) was used as precursor for TiO$_2$. All

11   model compounds, methyl orange, phenol red and sorbic acid used in the

12   photodegradation study were purchased from Sigma-Aldrich. LED strips were

13   purchased from LightingWill company with specifications of 24W 365 nm-370 nm UV

14   (Ultraviolet).

15   The supports used for immobilising TiO2 were obtained from different commercial

16   sources, as given below:

17   (1) Glass wool: Pyrex glass wool from Sigma-Aldrich

18   (2) Glass tape: Woven Glass Tape 1" Wide x 1/32" thick, manufactured by Wale

19   Apparatus and supplied by GPE Scientific Limited.

20   Both glass wool and glass tape were thermally pre-treated at 500 °C to burn off any

21   extraneous organic matter that may be present before subjecting to coating.

22

23   **Experimentation with dyes and sorbic acid**

24

25   **General procedures:**

26   Stock solutions of Phenol red, methyl orange and sorbic acid in double distilled water

27   were made so that the optical densities of the highest absorbing bands were

28   approximately 0.8. Then, 300 cm^3 of these solutions were used for photodegradation

29   experiments where the photo-reactor pods were immersed in the solutions and

30   subsequently irradiated. Samples were withdrawn at prescribed time intervals and

31   UV-Vis spectra were run on an Agilent UV-Visible spectrometer (model: UV-Vis-5000).

32   The degradations were monitored by the disappearance of the main bands with time.
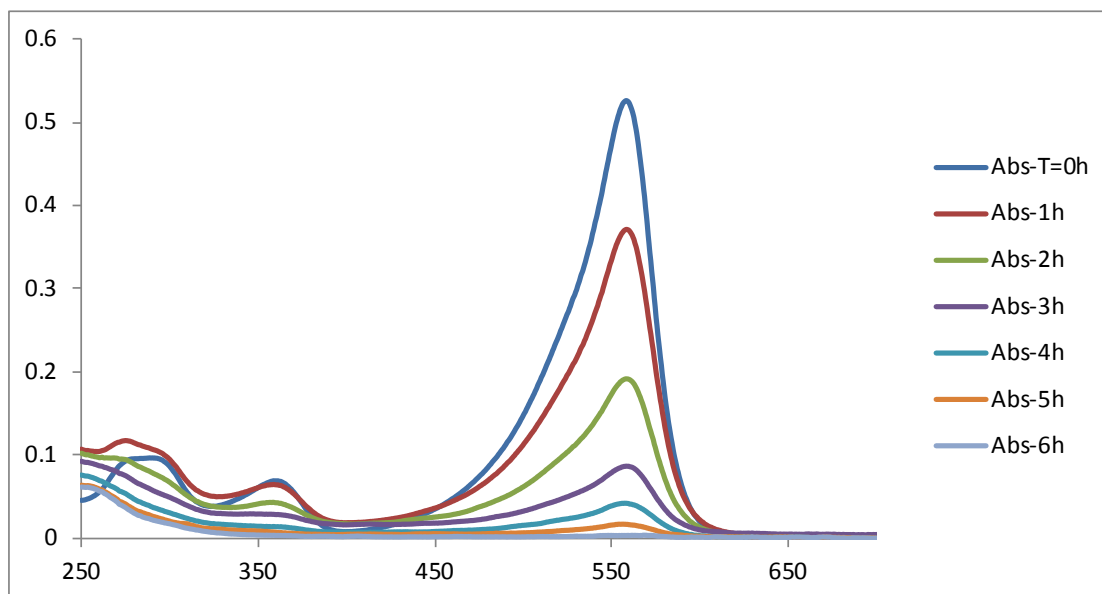
33

34

35   **Experiments with TiO$_2$ coated glass beads and dyes**
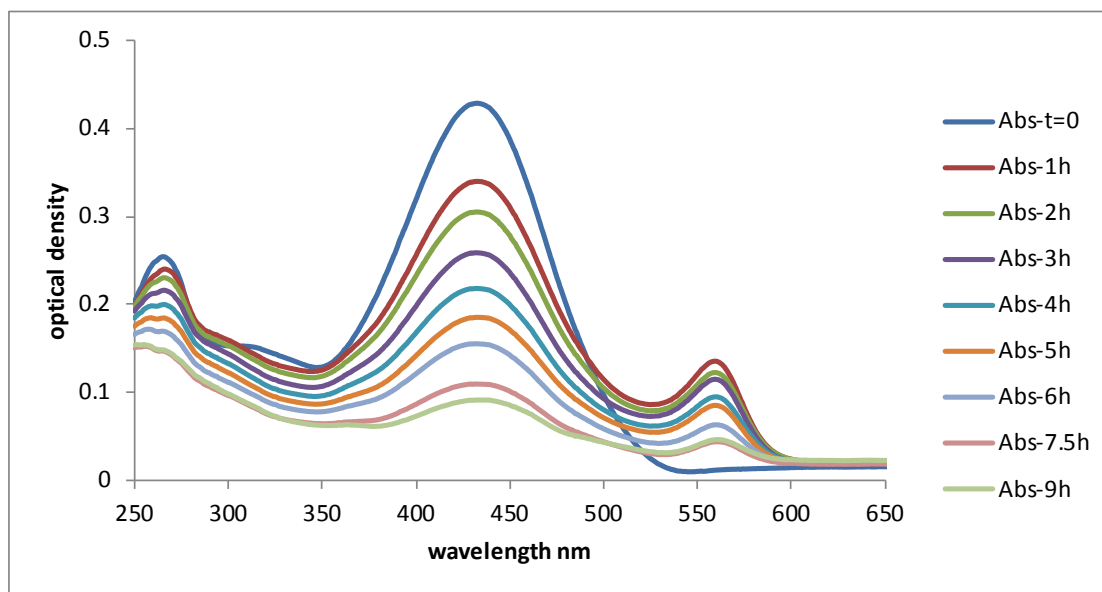
36

37   **Figure S1:** Photocatalytic degradation of phenol red withTiO$_2$ coated glass beads
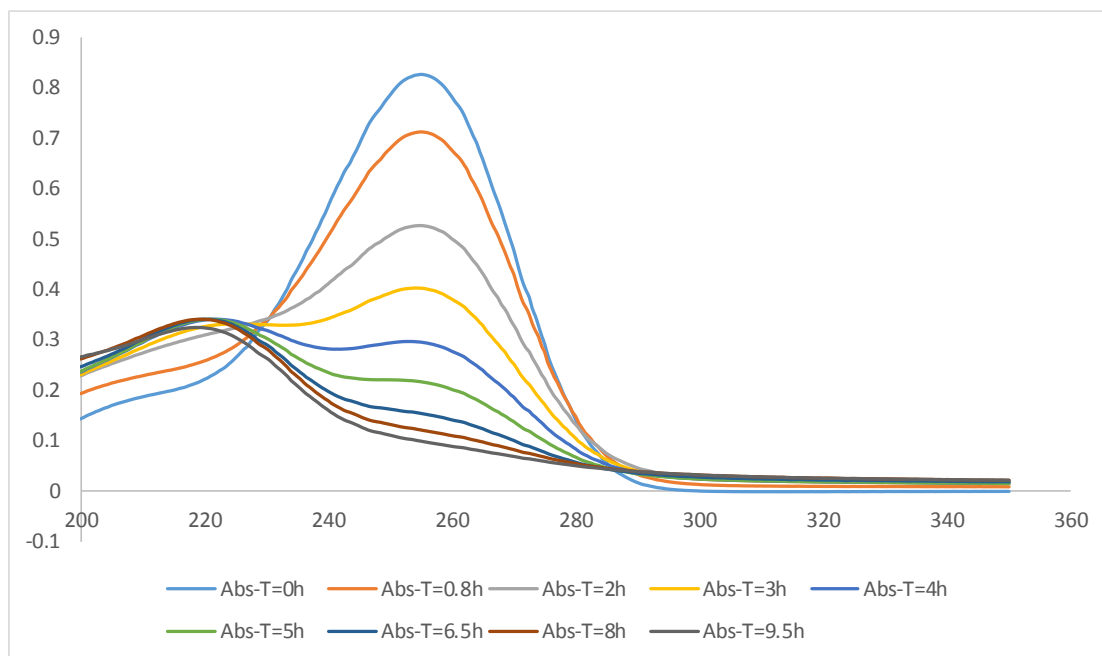
38

39

40   **Figure S2:** Photocatalytic degradation of phenol red withTiO$_2$ coated glass wool, carried out

41   under basic conditions(pH = 8.5)

42

43

44

45   **Figure S3:** Photocatalytic degradation of sorbic acid withTiO$_2$ coated glass wool, carried out

46   under neutral conditions(pH = 7.2)

47

48   **Preparation of TiO$_2$ coated glass beads:**

49   An infiltration method was employed to coat TiO$_2$ onto the porous glass beads. To

50   avoid catalyst shedding caused from glass beads breakage, the porous glass beads

51   were washed in acetone with ultrasonic treatment for 30 minutes. After that, a two-

52   hour calcination cycle at 550 °C was carried out to remove organic contamination on

53   the glass bead surface.

54   The precursor solution was prepared by adding 3.8 mL titanium (IV) isopropoxide into

55   10 mL isopropanol (Alfa Aesar, 99+%). After stirring for 30 minutes, the porous glass

56   beads were immersed into the precursor solution for 5 minutes. Infiltrated glass beads

57   were then dried in an oven at 80 °C. To increase the loading amount of the catalyst, a

58   repeated infiltration process was performed. After another drying step (80 ˚C), the

59   coated beads were calcined in a muffle furnace at 550 °C for 2 h to facilitate the

60   formation of anatase phase. The loading amount of TiO$_2$ is approximately 32 wt% after

61 two coating processes.

62 **Characterisation:**

63 The morphologies of uncoated and coated glass beads were observed by scanning

64 electron microscope (SEM, FEI Scios DualBeam) (Figure S4). Elemental analysis was

65 carried out on the same microscope working in energy dispersive X-ray spectroscopy

66 (EDX) mode.
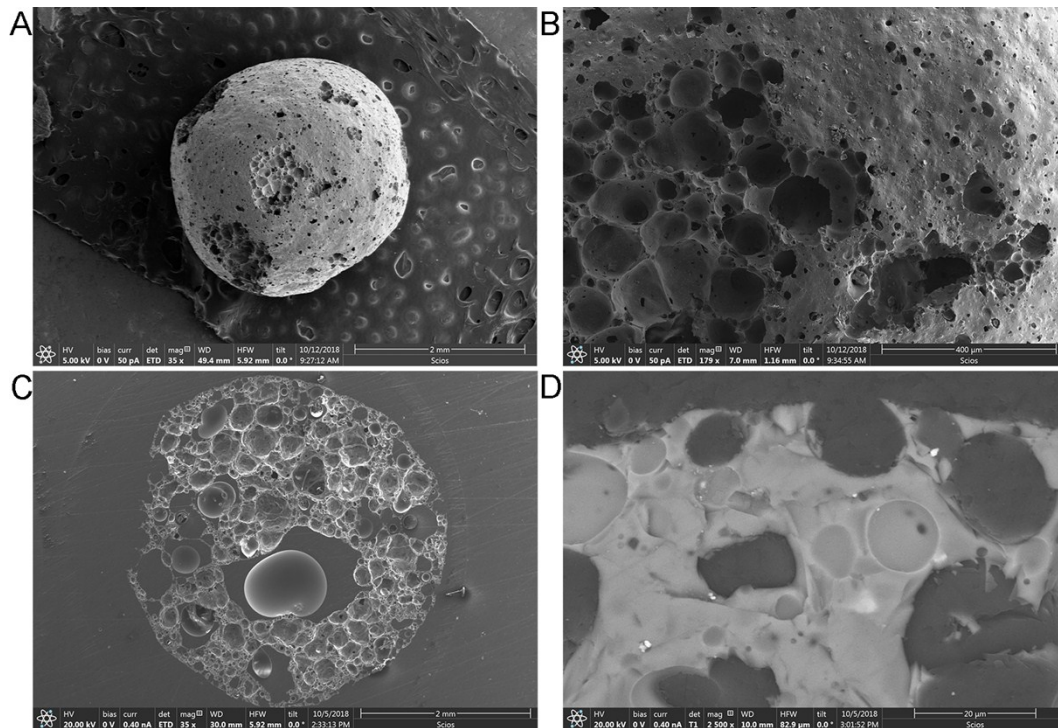
67

68

69 **Figure S4**: SEM images of uncoated glass beads: surface morphologies in low (A) and high (B)
70 magnifications; cross-section morphologies in low (C) and high (D) magnifications. Notes: Figure D is a
71 backscattering image, which shows bright contrast of a glass bead. The dark contrast in some pores
72 originates from resin used in sample preparation. It indicates that only parts of the pores are open so
73 that the liquid resin can penetrate to fill.

74

75 **Descriptions:** The porous glass beads have many pores with varying sizes. Most of the

76 pores are closed inside the bulk where solution cannot reach. This was illustrated by

77 backscattering image in Figure S4(D). However, those closed pores contribute to the

78 buoyancy of the glass beads.

79

80

81

82

Coating of glass wool and glass tapes

A measured quantity of glass wool (10 g) and glass tape (10 g) were dip coated once using a sol-gel solution of TiO_2 made using a standard method starting with $Ti(OiPr)_4$. Excess sol-gel solution was drained off, dried on filter paper and air dried in a fume hood overnight. Then both materials were calcined at 550 ˚C for 2 h to maximise the anatase phase formation. The TiO_2 loading was calculated taking into consideration the weight difference observed after coating. Glass tape contained 8.5 % w/w of TiO_2 while glass wool carried 7.2 % w/w. After calcination both materials were stored in a $CaCl_2$ desiccator.

92

Construction of photoreactor pods

The reactor pods were made from a fibre glass mesh with 4 mm x 4 mm holes attaching two LED strips (see Figure S5) to the inner wall with a silicone sealant. All the edges were sewn together with glass fibre thread. The unit was powered by a 12 DC V power supply.

Figure S5: Photograph of a LED strip used in this study. Forward voltage was 12 dcV and each pod typically has a current of 0.12 A, giving an overall power of 1.44 W (based on a 2-LED strip pod).

103

HPLC analysis of MC-LR

HPLC analysis was performed by using a Waters 2695 Separation Module. High resolution photodiode array detection was performed with a Waters 2996 Photodiode Array Detector (PDA). Separation of analytes was performed with a Symetry C18 column 2.1 mm (inner diameter) x 150 mm with a 5 µm particle size (all Waters, UK). The mobile phases used were ultrapure water and acetonitrile, both 0.05% TFA. Chromatography was achieved with a linear gradient from 15 to 75% acetonitrile over 10 minutes, followed by a solvent wash and equilibration. Column temperature was set to 40˚C and the flowrate applied was 0.3 mL min^{-1}. The resolution of the PDA was set to 1.2 nm and data was acquired over a range of 200 to 400 nm.

114

115